

Global Retrieval of 24-hourly Solar-Induced Chlorophyll Fluorescence and Evapotranspiration from OCO-2, OCO-3 and ECOSTRESS over 1982–2022

Zhuoying Deng^{1, 2}, Tingyu Li^{1, 2, #}, Jinghua Chen³, Shaoqiang Wang^{1, 2, 3, 4, *}, Kun Huang^{5, 6}, Peng Gu^{1, 2},
5 Haoyu Peng^{1, 2}, Zhihui Chen^{1, 2}

¹Hubei Key Laboratory of Regional Ecology and Environmental Change, School of Geography and Information Engineering, China University of Geosciences, Wuhan, Hubei, China

²Engineering Technology Innovation Center for Intelligent Monitoring and Spatial Regulation of Land Carbon Sinks, Ministry of Natural Resources, Wuhan, Hubei, China

10 ³Key Laboratory of Ecosystem Network Observation and Modeling, Institute of Geographic Sciences and Natural Resources Research, CAS, Beijing, China

⁴College of Resources and Environment, University of Chinese Academy of Sciences, Beijing, China

⁵Zhejiang Zhoushan Island Ecosystem Observation and Research Station, School of Ecological and Environmental Sciences, East China Normal University, Shanghai, China

15 ⁶Institute of Eco-Chongming (IEC), East China Normal University, Shanghai, China

*Correspondence to: Shaoqiang Wang (sqwang@igsnrr.ac.cn)

The author contributed equally to this work.

Supplementary material

Figure S1 to S7

20 Table S1 to S3

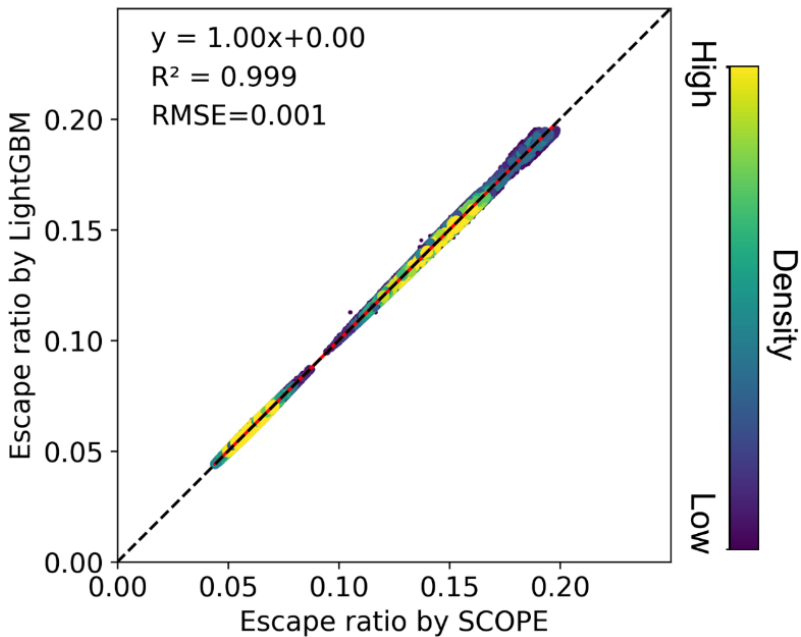


Figure S1 Validation of the LightGBM model on the SCOPE-simulated test set. A random selection of 20,000 sample points was used for plotting.

25

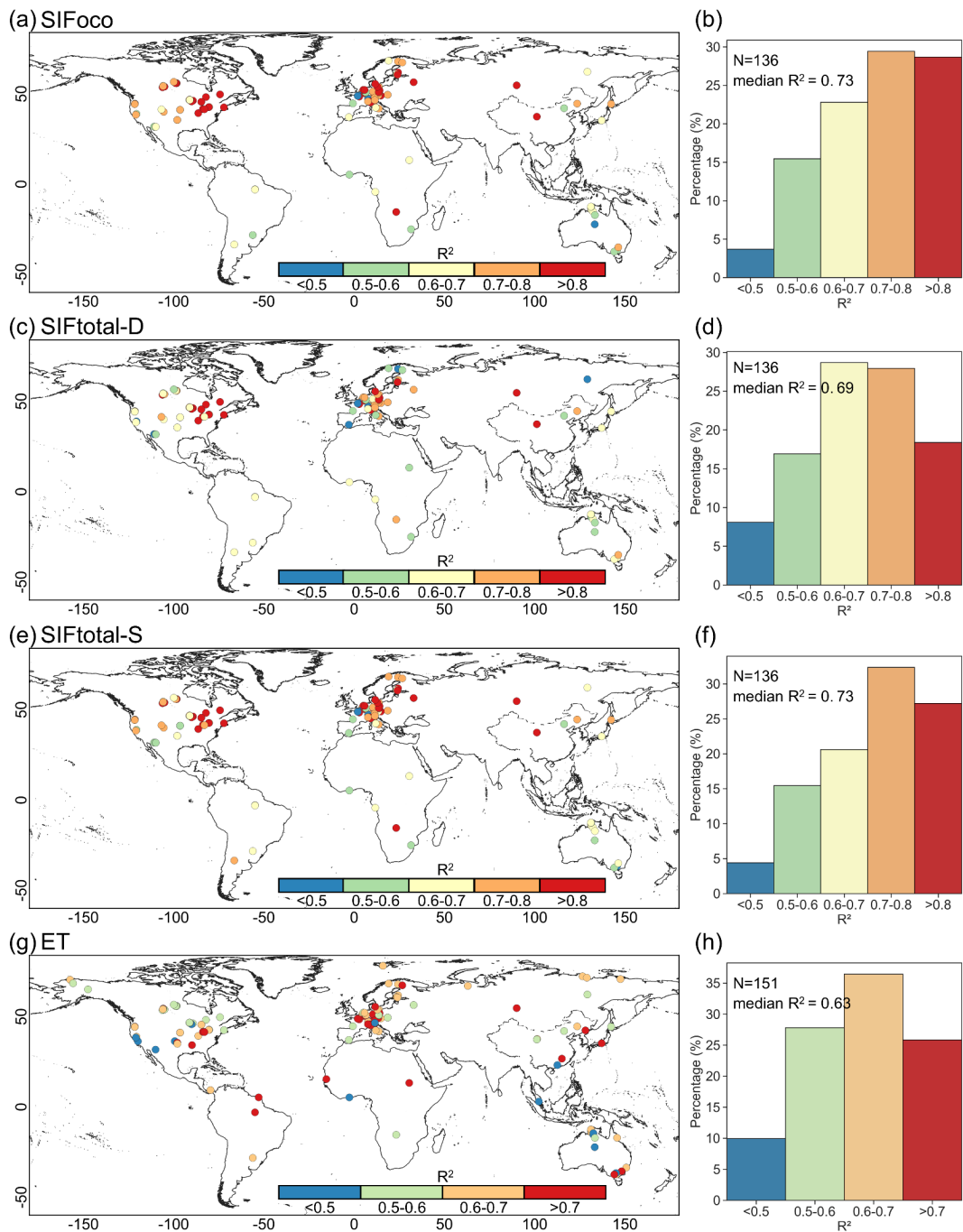


Figure S2 Validation of SIF and ET based on FLUXNET2015 sites. (a), (c), (e), and (g) show the global distribution of the coefficient of determination (R^2) for the comparisons of SIFOCO, SIFTOTAL-D, SIFTOTAL-S, and ET, respectively. Panels (b), (d), (f), and (h) present the statistical distribution of R^2 values for SIFOCO, SIFTOTAL-D, SIFTOTAL-S, and ET across these sites. All comparisons were conducted on the daily timescale.

30 In the daily-scale validation, additional sites were included due to the relaxation of quality control conditions.

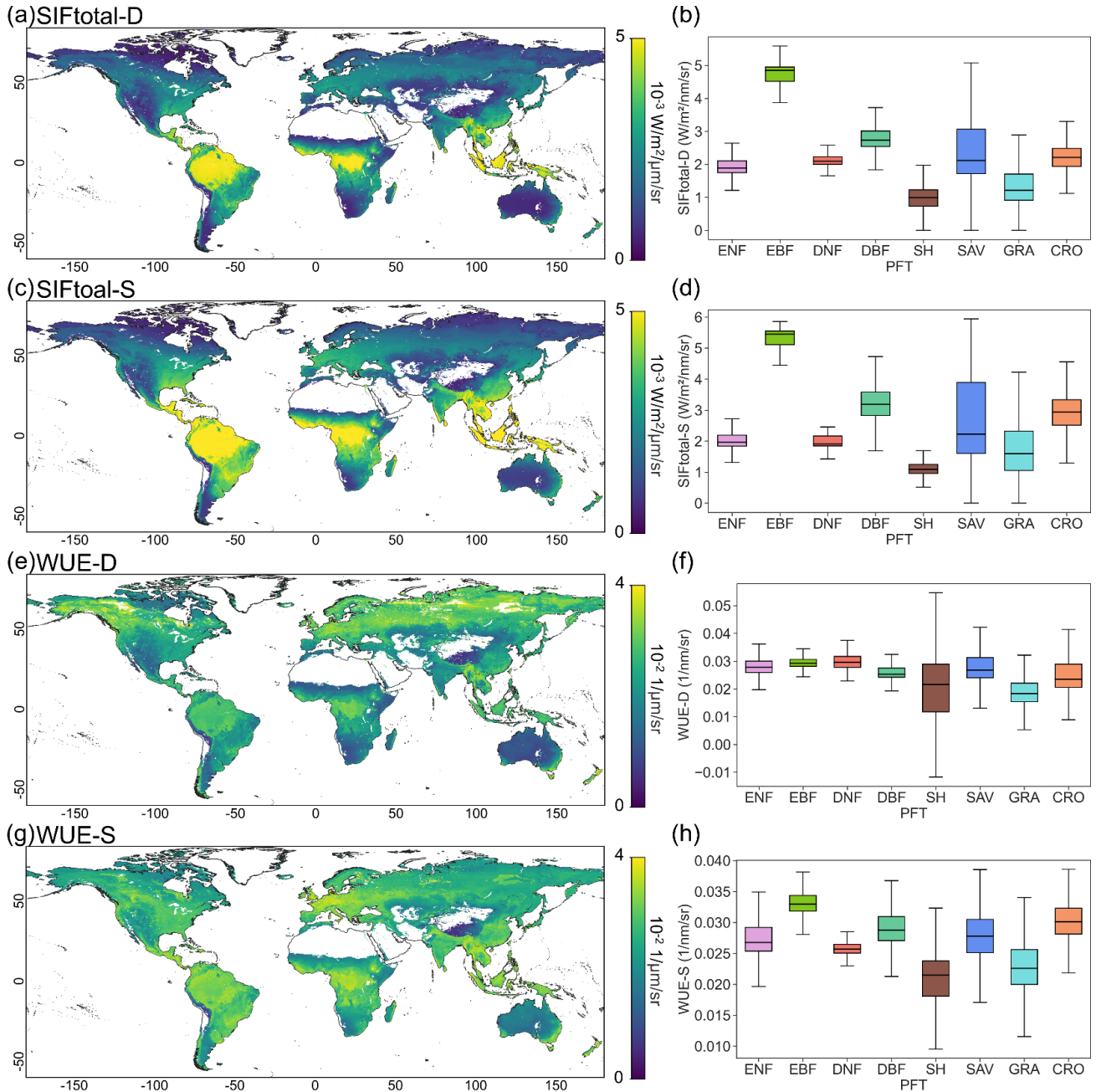
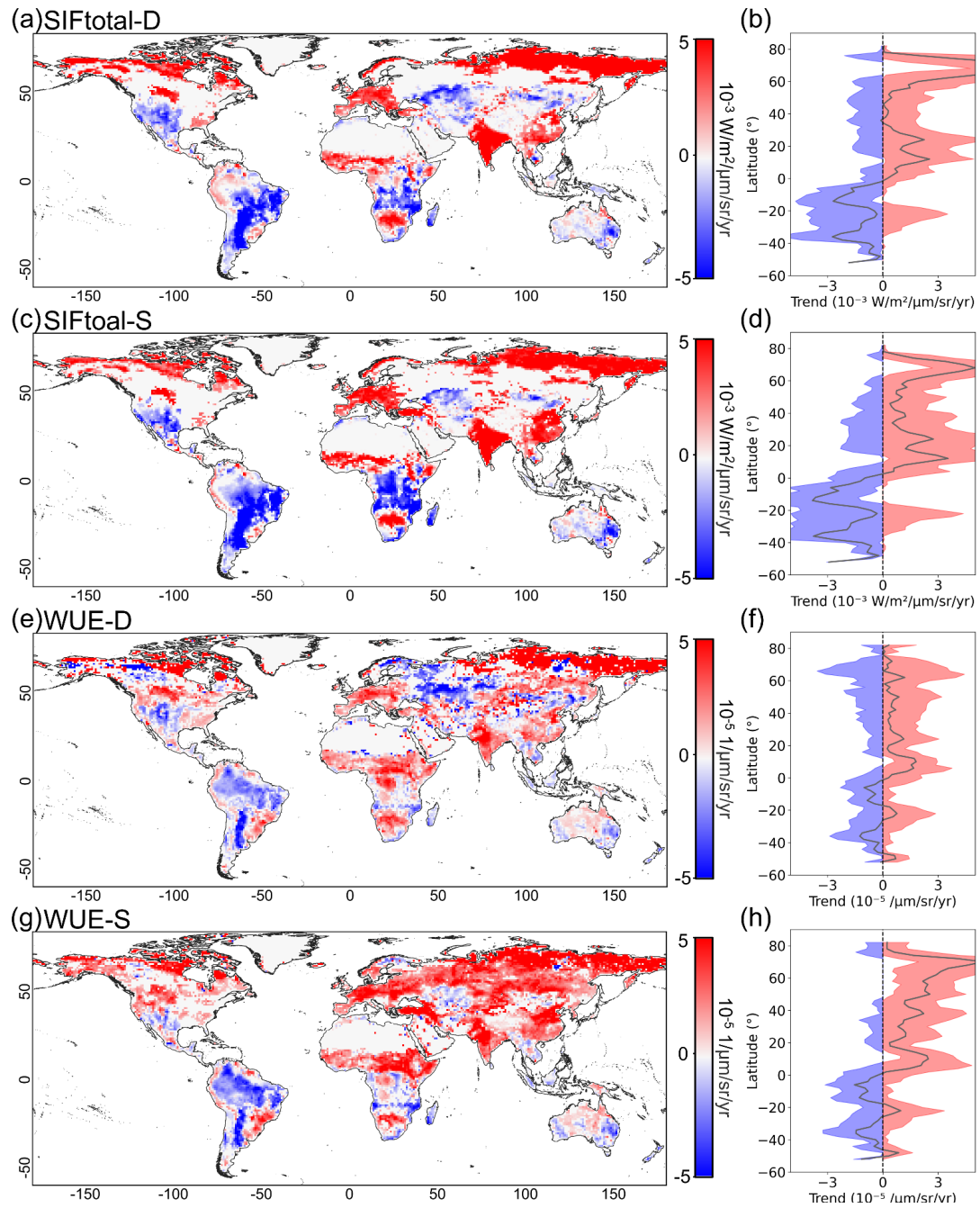
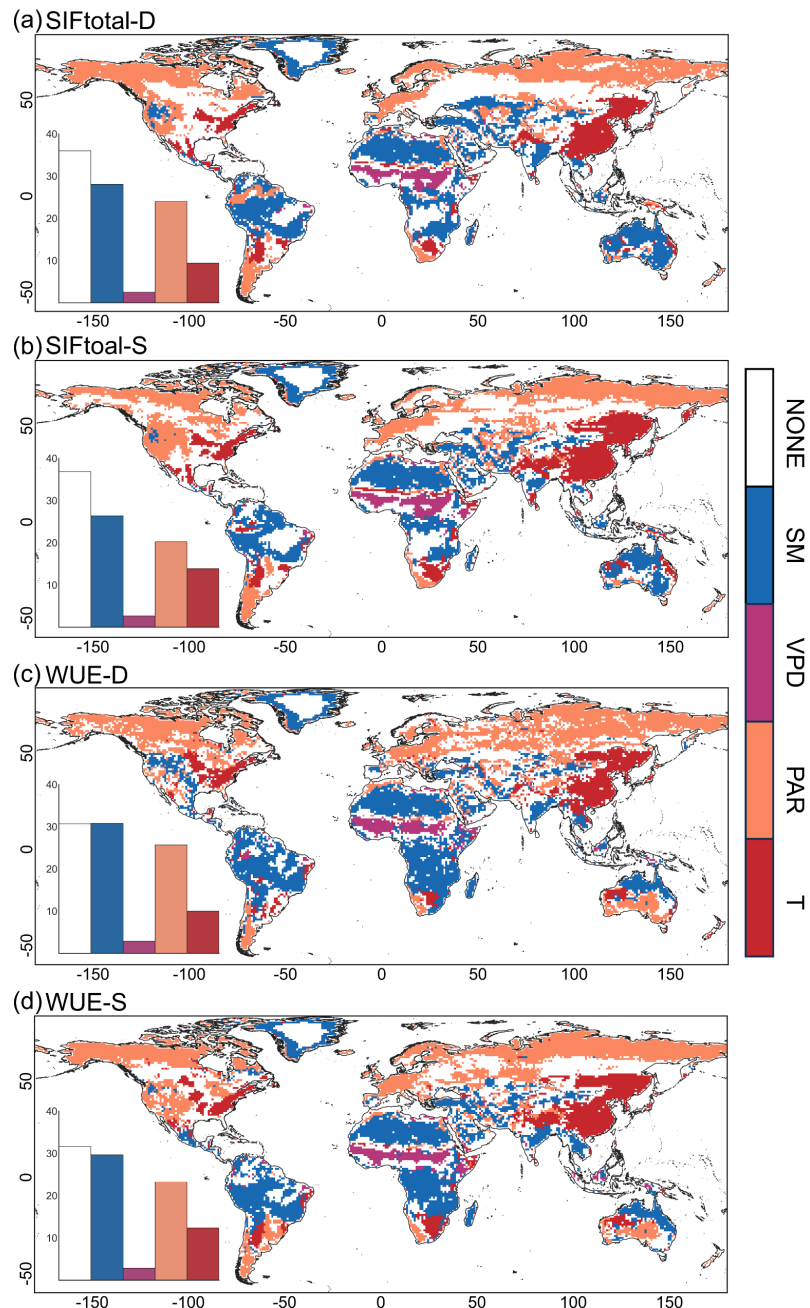


Figure S3 The spatial patterns of the mean values for global SIF_{total-D} (a), SIF_{total-S} (c), WUE-D (SIF_{total-D}/ET) (e), and WUE-S (SIF_{total-S}/ET) (g) from 1982 to 2022. The mean values of SIF_{total-D} (b), SIF_{total-S} (d), WUE-D (f), and WUE-S (h) are presented by plant functional types (PFTs): ENF represents evergreen needleleaf forests, EBF represents evergreen broadleaf forests, DNF represents deciduous needleleaf forests, DBF represents deciduous broadleaf forests, SH represents shrublands, SAV represents savannas, GRA represents grasslands, and CRO represents croplands.



40 **Figure S4** Trends of global SIF_{total}-D (a), SIF_{total}-S (c), WUE-D (SIF_{total}-D/ET) (e), and WUE-S (SIF_{total}-S/ET) (g) from 1982 to 2022. Trends were calculated on a per-pixel using linear regression. Pixels were retained for visualization only if they passed the 95% significance level of the Mann-Kendall trend test. The latitudinal profiles of the global average trends of SIF_{total}-D (b), SIF_{total}-S (d), WUE-D (f), and WUE-S (h) from 1982 to 2022, with shaded areas representing ± 1 standard deviation.



45

50

Figure S5 Dominant factor analysis for SIF_{total}-D (a), SIF_{total}-S (b), WUE-D (SIF_{total}-D/ET) (c), and WUE-S (SIF_{total}-S/ET) (d) based on the SURD algorithm. Blue pixels represent dominance by soil moisture (SM), purple pixels indicate dominance by VPD, orange pixels represent dominance by PAR, red pixels indicate dominance by air temperature (T), and white pixels indicate there is no dominant factor. Calculations were performed using daily-aggregated data from 1982 to 2022. The bar chart in each map represents the proportion of pixels dominated by each factor.

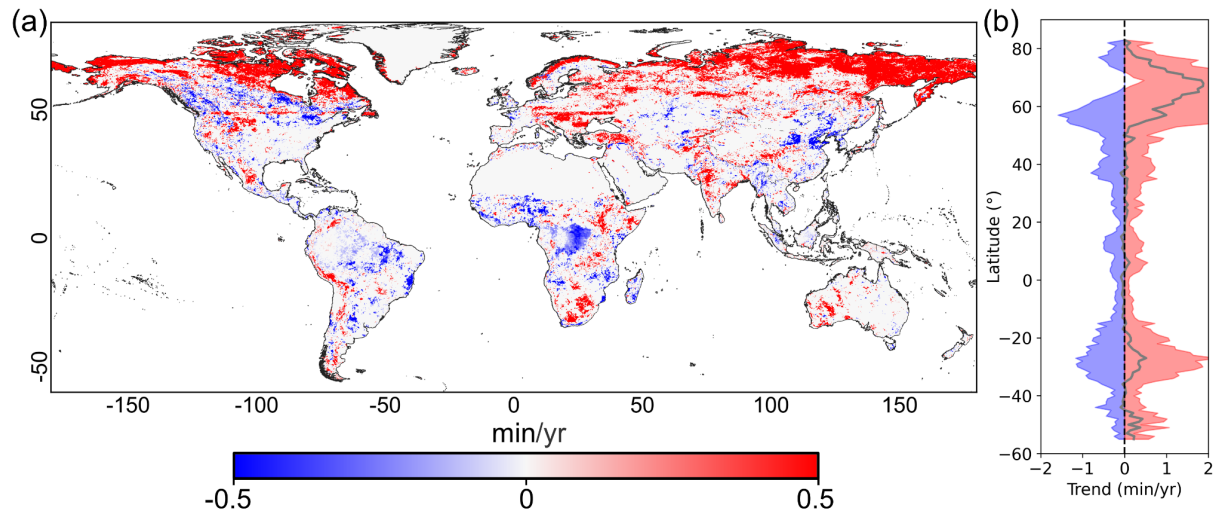


Figure S6 (a) Trends of the peak timing of SIF during the day from 1982 to 2022. Trends were calculated on a per-pixel using linear regression. Pixels were retained for visualization only if they passed the 95% significance level of the Mann-Kendall trend test. (b) The
55 latitudinal profiles of the global average trends from 1982 to 2022, with shaded areas representing ± 1 standard deviation.

60

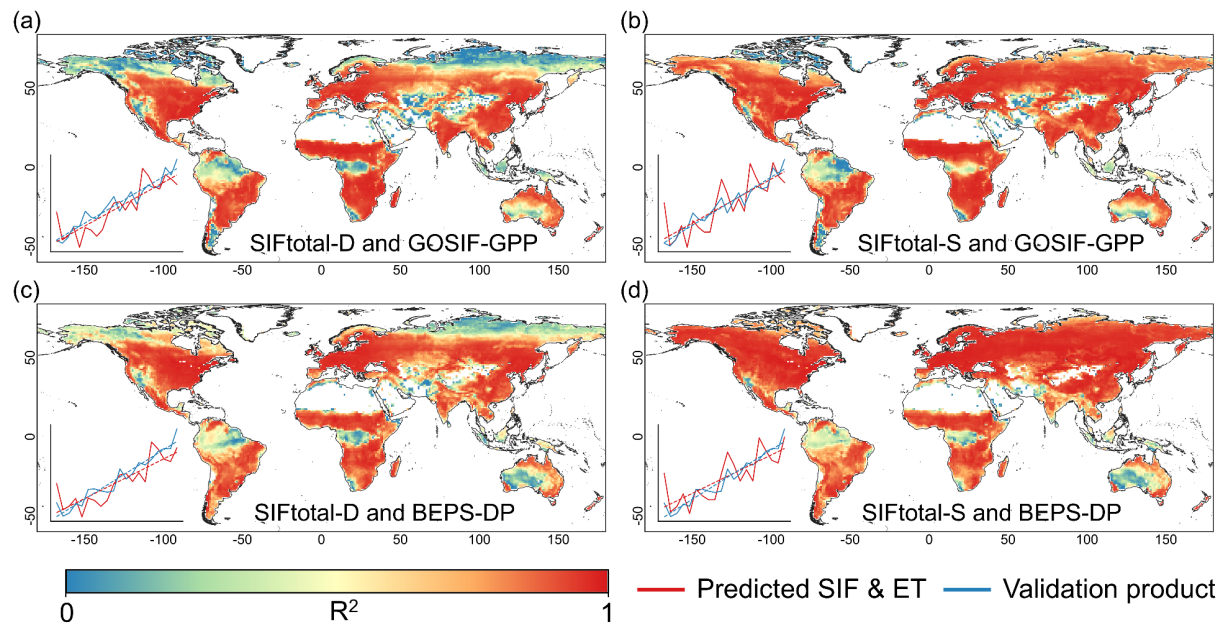


Figure S7 Validation of two SIF_{total} data based on global gridded GPP products. (a) and (b) represent the validation of $SIF_{total\text{-}D}$ and $SIF_{total\text{-}S}$ using GOSIF-GPP (from 2001 to 2022), respectively. (c) and (d) represent the validation using BEPS-DP (from 2001 to 2020). All comparisons were conducted based on the R^2 of the monthly time series for each grid cell. The plot in the bottom-left corner of each map illustrates the long-term global grid-averaged normalized trends for predicted data (red) and the validation products (blue). The global mean was calculated using area-weighted averaging based on grid sizes.

70

75

80

85

8

Table S1: FLUXNET2015 sites used for the validation of SIF and ET data.

Site name	Longitude (°)	Latitude (°)	Used to validate SIF or ET
AR-SLu	-66.4598	-33.4648	SIF
AR-Vir	-56.1886	-28.2395	SIF and ET
AT-Neu	11.3175	47.11667	SIF
AU-Ade	131.1178	-13.0769	SIF and ET
AU-Cpr	140.5891	-34.0021	SIF and ET
AU-Cum	150.7236	-33.61518	SIF and ET
AU-DaP	131.3181	-14.0633	SIF and ET
AU-DaS	131.3881	-14.1593	SIF and ET
AU-Dry	132.3706	-15.2588	SIF and ET
AU-Emr	148.4746	23.8587	ET
AU-Fog	131.3072	-12.5452	SIF and ET
AU-Gin	115.7138	-31.3764	SIF and ET
AU-GWW	120.6541	-30.1913	SIF and ET
AU-How	131.1523	-12.4943	SIF and ET
AU-RDF	132.4776	-14.5636	ET
AU-Rig	145.5759	-36.6499	SIF and ET
AU-Rob	145.6301	-17.1175	SIF and ET
AU-Stop	133.3502	-17.1507	ET
AU-Tum	148.1517	-35.6566	SIF and ET
AU-Wac	145.1878	-37.4259	SIF and ET
AU-Whr	145.0294	-36.6732	SIF and ET
AU-Wom	144.0944	-37.4222	SIF and ET
AU-Ync	146.2907	-34.9893	SIF and ET
BE-Bra	4.51984	51.30761	SIF and ET
BE-Lon	4.74623	50.55162	SIF
BE-Vie	5.99812	50.30493	SIF and ET
BR-Sa1	-54.9589	-2.85667	SIF and ET
BR-Sa3	-54.9714	-3.01803	SIF and ET
CA-Gro	-82.1556	48.2167	SIF
CA-Man	-98.4808	55.87962	SIF and ET
CA-NS1	-98.4839	55.87917	SIF and ET

CA-NS2	-98.5247	55.90583	SIF and ET
CA-NS3	-98.3822	55.91167	SIF and ET
CA-NS4	-98.3806	55.91437	SIF and ET
CA-NS5	-98.485	55.86306	SIF and ET
CA-NS6	-98.9644	55.91667	SIF and ET
CA-NS7	-99.94833	56.63583	ET
CA-Oas	-106.198	53.62889	SIF
CA-Obs	-105.118	53.98717	SIF
CA-Qfo	-74.3421	49.6925	SIF and ET
CA-SF1	-105.818	54.48503	SIF and ET
CA-SF2	-105.878	54.25392	SIF and ET
CA-SF3	-106.00526	54.09156	ET
CA-TP1	-80.5595	42.66093611	SIF and ET
CA-TP2	-80.4588	42.77441944	ET
CA-TP3	-80.3483	42.70681111	ET
CA-TP4	-80.3574	42.710161	SIF and ET
CA-TPD	-80.5577	42.635328	SIF and ET
CG-Tch	11.65642	-4.28917	SIF and ET
CH-Cha	8.41044	47.21022	SIF and ET
CH-Dav	9.85591	46.81533	SIF
CH-Fru	8.53778	47.11583	SIF and ET
CH-Lae	8.36439	47.47833	SIF and ET
CH-Oe1	7.73194	47.28583	SIF and ET
CH-Oe2	7.73375	47.28642	SIF and ET
CN-Cha	8.41044	47.21022	ET
CN-Cng	123.5092	44.5934	SIF and ET
CN-Din	112.5361	23.1733	ET
CN-Du2	116.2836	42.0467	ET
CN-Ha2	101.3269	37.6086	ET
CN-HaM	101.18	37.37	SIF and ET
CN-Qia	115.0581	26.7414	ET
CZ-BK1	18.53688	49.50208	SIF and ET
CZ-BK2	18.54285	49.49443	SIF

CZ-wet	14.77035	49.02465	SIF and ET
DE-Akm	13.68342	53.86617	SIF and ET
DE-Geb	10.91463	51.09973	SIF and ET
DE-Gri	13.51253	50.94947	SIF and ET
DE-Hai	10.45217	51.07921	SIF and ET
DE-Kli	13.52238	50.89306	SIF
DE-Lkb	13.30467	49.09962	SIF and ET
DE-Lnf	10.3678	51.32822	SIF and ET
DE-Obe	13.72129	50.78666	SIF and ET
DE-RuR	6.30413	50.62191	SIF and ET
DE-RuS	6.44717	50.86591	SIF and ET
DE-Seh	6.44965	50.87062	SIF and ET
DE-SfN	11.3275	47.80639	SIF and ET
DE-Spw	14.03369	51.89225	SIF and ET
DE-Tha	13.56515	50.96256	SIF and ET
DE-Zrk	12.88901	53.87594	SIF and ET
DK-Fou	9.58722	56.4842	SIF
DK-Sor	11.64464	55.48587	SIF and ET
ES-LgS	-2.96583	37.09794	SIF and ET
ES-LJu	-2.75212	36.92659	ET
FI-Hyy	24.29477	61.84741	SIF and ET
FI-Jok	23.51345	60.8986	SIF and ET
FI-Let	23.95952	60.64183	SIF and ET
FI-Lom	24.20918	67.99724	ET
FI-Sod	26.63859	67.36239	SIF and ET
FR-Fon	2.7801	48.47636	SIF and ET
FR-Gri	1.95191	48.84422	SIF
FR-LBr	-0.7693	44.71711	SIF and ET
FR-Pue	3.5957	43.7413	SIF and ET
GF-Guy	-52.9249	5.27877	SIF and ET
GH-Ank	-2.69421	5.26854	SIF
IT-CA1	12.02656	42.38041	SIF and ET
IT-CA2	12.02604	42.37722	ET

IT-CA3	12.0222	42.38	SIF and ET
IT-Col	13.58814	41.84936	SIF and ET
IT-Isp	8.63358	45.81264	SIF and ET
IT-La2	11.2853	45.9542	SIF
IT-Lav	11.28132	45.9562	SIF and ET
IT-MBo	11.04583	46.01468	SIF and ET
IT-PT1	9.06104	45.20087	SIF and ET
IT-Ren	11.43369	46.58686	SIF
IT-Ro1	11.93001	42.40812	SIF and ET
IT-Ro2	11.92093	42.39026	SIF and ET
IT-Tor	7.57806	45.84444	SIF and ET
JP-MBF	142.3186	44.3869	SIF
JP-SMF	137.0788	35.2617	SIF and ET
MY-PSO	102.3062	2.973	ET
NL-Hor	5.0713	52.24035	SIF and ET
NL-Loo	5.74356	52.16658	SIF and ET
PA-SPn	-79.6346	9.31814	SIF and ET
PA-SPs	-79.6314	9.31378	SIF and ET
RU-Cok	147.4943	70.82914	ET
RU-Fyo	32.92208	56.46153	SIF
RU-Ha1	90.00215	54.72517	SIF and ET
RU-Sam	126.4978	72.3733	ET
RU-Vrk	62.94047	67.05468	ET
SD-Dem	30.4783	13.2829	ET
SN-Dhr	-15.4322	15.40278	ET
US-AR1	-99.42	36.4267	ET
US-AR2	-99.5975	36.6358	ET
US-ARB	-98.0402	35.5497	SIF and ET
US-ARc	-98.04	35.54649	SIF and ET
US-ARM	-97.4888	36.6058	ET
US-Atq	-157.409	70.4696	ET
US-Blo	-120.633	38.8953	SIF and ET
US-CRT	-83.3471	41.628495	ET

US-Goo	-89.8735	34.2547	ET
US-Ha1	-72.1715	42.5378	SIF and ET
US-Lin	-119.842	36.3566	ET
US-Los	-89.9792	46.0827	SIF
US-LWW	-97.9789	34.9604	ET
US-Me1	-121.5	44.5794	SIF
US-Me2	-121.557	44.4523	SIF and ET
US-Me3	-121.608	44.3154	SIF and ET
US-Me5	-121.567	44.43719	SIF and ET
US-Me6	-121.608	44.3232842	SIF and ET
US-MMS	-86.4131	39.3232	SIF and ET
US-Ne1	-96.4766	41.16506	SIF and ET
US-Ne2	-96.4701	41.16487	SIF and ET
US-Ne3	-96.4397	41.17967	SIF and ET
US-NR1	-105.546	40.0329	SIF
US-Oho	-83.8438	41.5545	SIF and ET
US-PFa	-90.2723	45.9459	SIF
US-SRC	-110.8395	31.9083	ET
US-SRG	-110.827675	31.789379	ET
US-SRM	-110.8661	31.8214	ET
US-Syv	-89.3477	46.242	SIF
US-Ton	-120.966	38.4316	SIF and ET
US-UMB	-84.7138	45.5598	SIF and ET
US-UMd	-84.6975	45.5625	SIF and ET
US-WCr	-90.0799	45.8059	SIF
US-Wi0	-91.0814	46.618778	SIF and ET
US-Wi1	-91.2329	46.730472	SIF and ET
US-Wi2	-91.1528	46.686889	SIF and ET
US-Wi3	-91.0987	46.634722	SIF and ET
US-Wi4	-91.1663	46.739333	SIF and ET
US-Wi5	-91.0858	46.653083	SIF and ET
US-Wi6	-91.2982	46.624889	SIF and ET
US-Wi7	-91.0693	46.649111	SIF and ET

US-Wi8	-91.2524	46.722333	SIF and ET
US-Wi9	-91.0814	46.618778	SIF and ET
US-WPT	-82.9962	41.464639	SIF and ET
ZA-Kru	31.4969	-25.0197	SIF and ET
ZM-Mon	23.2525	-15.4391	SIF and ET

90

95

100

105

110

115

14

Table S2: Flux sites used for the validation of SIF diurnal variations.

Site name	Longitude (°)	Latitude (°)	Reference
Ames	-93.6936	41.9747	Magney et al., 2019a
Niwot Ridge	-105.55	40.03	Magney et al., 2019b
Ca-obs	-105.12	53.98	Chen et al., 2024
Yangling 1–Yangling 5	108.07	34.28	Liu et al., 2022

120

125

130

135

140

15

145 **Table S3:** Input parameters and values set in LightGBM model for the fusion of OCO-2 and OCO-3 SIF.

Parameter	Symbol	Parameter	Symbol
OCO-2 Observed SIF	SIFoco-2	Continuum Level Radiance at 771 nm	L771
Solar Zenith Angle	SZA	Percentage of land surface type within the sounding	Land_Fract
Solar Azimuth Angle	SAA	Skin temperature at the sounding location	TEM_Skin
View Zenith Angle	VZA	Two-meter temperature at the sounding location	TEM_2m
View Azimuth Angle	VAA	Vapour pressure deficit at the sounding location (2m)	VPD
Surface Albedo	Albedo	Specific humidity at surface layer at the sounding location	Humidity
Ratio of retrieved and predicted O ₂ column in the 771 nm window	O ₂	Surface wind speed at sounding location	Wind_Speed
Ratio of CO ₂ retrieved in weak and strong CO ₂ band	CO ₂	Surface pressure at the sounding location	Pressure
Retrieved-predicted surface pressure from ABO2	Pressure_A	Longitude	Lon
Continuum Level Radiance at 757 nm	L757	Latitude	Lat